

# Detection of Carboxylesterase 1 and Chlorpyrifos with ZIF-8 Metal–Organic Frameworks Using a Red Emission BODIPY-Based Probe

Baoxing Shen,\* Chenggong Ma, Yuan Ji, Jianan Dai, Bingzhi Li, Xing Zhang,\* and He Huang\*



Cite This: *ACS Appl. Mater. Interfaces* 2021, 13, 8718–8726



Read Online

ACCESS |

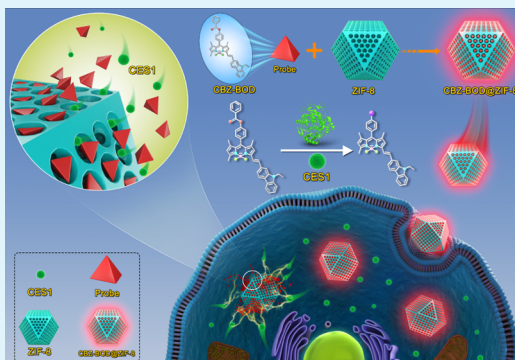
Metrics & More

Article Recommendations

Supporting Information

**ABSTRACT:** In this work, a red emission fluorescent probe CBZ-BOD@zeolitic imidazolate framework-8 (ZIF-8) was fabricated based on metal–organic frameworks (MOFs) for detecting carboxylesterase 1 (CES1). The small molecule probe CBZ-BOD was first synthesized and then used to prepare the functionalized MOF material. ZIF-8 was chosen as an encapsulation shell to improve the detection properties of CBZ-BOD. Using this unique porous materials, ultrasensitive quantification of CES1 and chlorpyrifos was successfully realized. The low detection limit and high fluorescence quantum yield were calculated as 1.15 ng/mL and 0.65 for CBZ-BOD@ZIF-8, respectively. CBZ-BOD@ZIF-8 has good biocompatibility and was successfully applied to monitor the activity of CES1 in living cells. A molecular docking study was used to explore the binding of CES1 and CBZ-BOD, finding that CES1 can bind with the probe before and after hydrolysis. This type of materialized probe can inspire the development of fluorescent tools for further exploration of many pathological processes.

**KEYWORDS:** red emission, metal–organic frameworks, molecular docking, carboxylesterase 1, pesticide detection



## 1. INTRODUCTION

Over the past few decades, the wide use of agricultural pesticides has indeed significantly increased the food production.<sup>1–4</sup> However, the accumulation of these artificial chemicals would cause serious environmental pollution and risk human health.<sup>5–7</sup> Although pesticide residues exist in different media, they will eventually enter the final media human body through food chains and lead to many diseases including cancer, deformities, and genetic mutagenesis.<sup>8–10</sup> Besides, some pesticide residues can also affect the nervous system and immune system.<sup>11,12</sup> Thus, developing methods that can effectively detect pesticide residues is of great significance.<sup>13–16</sup>

Great efforts have been made to develop effective methods for the determination of pesticide residues in the media that they may occur.<sup>17–20</sup> For example, high performance liquid chromatography, gas chromatography/mass spectrometry, and electrochemical analysis.<sup>21–23</sup> Although these methods are sensitive enough for the detection of pesticides in complex samples, they involve expensive instruments, complex sample pretreatment, and the need for skilled operators.<sup>24–26</sup> Therefore, wide application of these methods in *in situ* rapid detection is limited. Fluorescent probes based on the inhibition of enzyme activity have shown satisfactory results for pesticide analysis.<sup>27–29</sup> Although fluorescent probes have the advantages of low cost, rapid detection, and simple operation, there still remain challenges with organic small molecule enzyme probes

like high detection limit (LOD), poor selectivity, and solubility.<sup>30–33</sup>

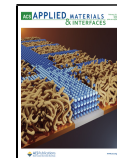
In recent years, metal organic framework (MOF) materials have been extensively applied to various fields such as chemical catalysis, gas separation, biosensors, and detection as well as drug delivery due to their excellent properties including large specific surface area, adjustable topology, uniform aperture size, rich binding interaction for the selected reagents, excellent photoelectric properties, and high stability. At present, it is very rarely reported that MOF materials are used to encapsulate the organic small molecule fluorescent probe to improve the detection properties. Thus, we encapsulate the probe in the MOF material for the purpose of improving the tolerability, stability, and biocompatibility of the probe, which can contribute to the improvement of detection performance.

Herein, we designed a novel fluorogenic platform in which zeolitic imidazolate framework-8 (ZIF-8) was used as a carrier to encapsulate a red emission carboxylesterase 1 (CES1)-specific binding small-molecule probe for quantitative determination of CES1. In this work, a red emission organic small

Received: November 5, 2020

Accepted: February 2, 2021

Published: February 11, 2021

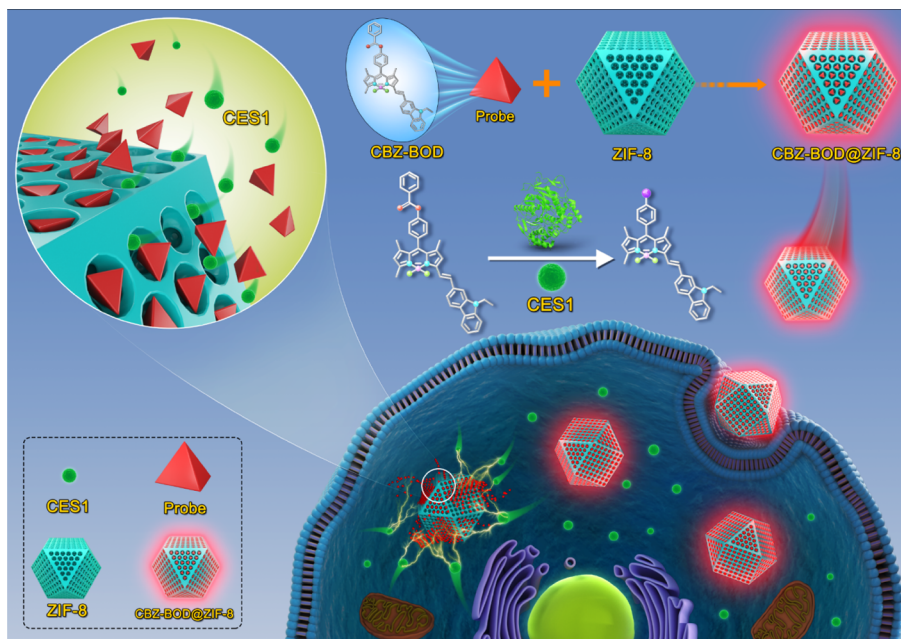


ACS Publications

© 2021 American Chemical Society

8718

<https://dx.doi.org/10.1021/acsami.0c19811>  
*ACS Appl. Mater. Interfaces* 2021, 13, 8718–8726

**Scheme 1.** Designing of CBZ-BOD@ZIF-8 and Its Applications in Living Cell Detection

molecular probe CBZ-BOD was first synthesized (Scheme 1). Molecular docking results suggest that CBZ-BOD can have a specific response to CES1 through the binding effect and is accompanied with a significant fluorescence change. Then, CBZ-BOD@ZIF-8 was prepared for sensitively monitoring CES1 activities in the presence or absence of chlorpyrifos. The results show that CBZ-BOD@ZIF-8 has better sensitivity, and the low LOD was calculated as 1.15 ng/mL. In addition, CBZ-BOD@ZIF-8 showed good biocompatibility and was successfully applied to achieve the visual monitoring of CES1 activity in living cells. This type of probe can inspire the development of fluorescent tools for further exploration of many pathological processes.

## 2. SYNTHESIS AND METHODS

**2.1. Compound BOD-OH.** Under a nitrogen atmosphere, compound 1 (0.62 mmol, 0.21 g) was dissolved using 15 mL of toluene in an oil–water separator, then followed by adding *n*-ethylcarbazole-3-formaldehyde (3.09 mmol, 0.69 g) and *p*-toluene sulfonic acid (0.83 mmol, 0.14 g), and 650  $\mu$ L of piperidine was added last. Then, the reaction mixture was refluxed at 110 °C overnight. After the reaction was finished, the mixture solution turned blue-black, and a strong red fluorescence was observed using thin-layer chromatography. The reaction solution was extracted with 20 mL of dichloromethane (DCM) and 40 mL of water three times. The separated organic fraction was dried over anhydrous sodium sulfate. After vacuum concentration, the blue-purple solid was purified by column chromatography to obtain BOD-OH.  $^1\text{H}$  NMR (400 MHz,  $\text{CDCl}_3$ ):  $\delta$  8.32 (s, 1H), 8.20 (d,  $J$  = 7.7 Hz, 1H), 7.84–7.73 (m, 2H), 7.50 (dd,  $J$  = 8.4, 7.4 Hz, 2H), 7.43 (dd,  $J$  = 13.8, 8.3 Hz, 2H), 7.34–7.27 (m, 2H), 7.17 (d,  $J$  = 8.5 Hz, 2H), 6.99 (d,  $J$  = 8.5 Hz, 2H), 6.68 (s, 1H), 6.02 (s, 1H), 4.40 (q,  $J$  = 7.2 Hz, 2H), 2.66 (s, 3H), 1.53 (s, 3H), 1.48 (s, 6H).  $^{13}\text{C}$  NMR (101 MHz, DMSO):  $\delta$  158.61, 153.74, 153.54, 143.09, 141.90, 141.07, 140.83, 140.59, 140.58, 139.14, 133.26, 131.83, 129.80, 129.30, 127.72, 126.81, 125.38, 125.00, 123.26, 122.63, 121.38, 121.16, 120.74, 119.97, 118.49, 116.53, 115.73, 114.41, 110.44, 110.06, 49.11, 40.62, 40.41, 40.20, 37.73, 31.65, 30.34, 14.98, 14.82, 14.62, 14.25.  $\text{C}_{34}\text{H}_{29}\text{BF}_2\text{N}_3\text{O}_2^+$ , Calcd: 544.5; Obsd: 544.5.

**2.2. Compound CBZ-BOD.** The purified BOD-OH (80.00 mg, 0.15 mmol) was dissolved by DCM (15 mL) in a 100 mL round

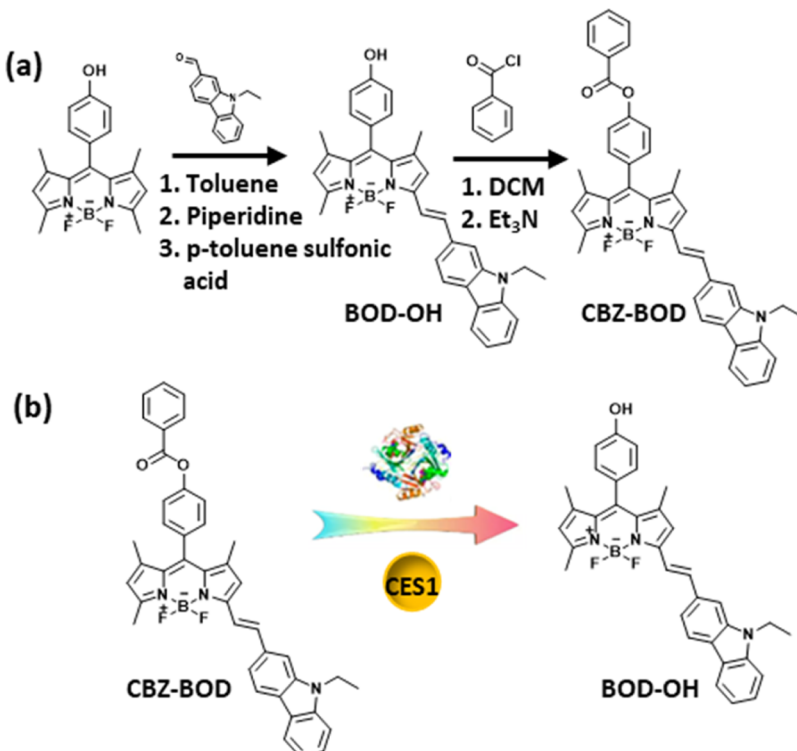
bottom flask, and triethylamine (30.60  $\mu$ L, 0.22 mmol) was added into the flask subsequently. Finally, benzoyl chloride (34.00  $\mu$ L, 0.29 mmol) was added drop by drop. The mixture was stirred overnight at room temperature. After the reaction was finished, the reaction mixture was concentrated and raw product was purified by column chromatography to obtain a purplish black solid.  $^1\text{H}$  NMR (400 MHz,  $\text{CDCl}_3$ ):  $\delta$  8.34 (s, 1H), 8.27 (t,  $J$  = 6.5 Hz, 2H), 8.20 (d,  $J$  = 7.7 Hz, 1H), 8.17–8.13 (m, 4H), 7.65 (t,  $J$  = 7.4 Hz, 2H), 7.59 (d,  $J$  = 7.9 Hz, 2H), 7.52 (s, 2H), 7.43 (s, 4H), 6.74 (s, 1H), 6.05 (d,  $J$  = 9.2 Hz, 1H), 4.42 (q,  $J$  = 7.2 Hz, 2H), 2.68 (s, 3H), 1.59 (s, 3H), 1.54 (s, 3H), 1.50 (d,  $J$  = 7.1 Hz, 3H).  $^{13}\text{C}$  NMR (101 MHz, DMSO):  $\delta$  167.85, 167.51, 165.58, 164.93, 151.71, 140.90, 140.59, 133.34, 132.39, 132.22, 132.06, 131.25, 130.35, 130.10, 129.95, 129.74, 129.51, 129.30, 129.27, 129.13, 129.04, 129.03, 129.02, 129.01, 129.00, 128.87, 127.65, 127.02, 125.43, 123.44, 123.27, 122.63, 120.86, 114.42, 49.08, 31.60, 30.30, 29.48, 28.85, 23.75, 22.87, 14.33, 14.21, 11.36, 11.25.  $\text{C}_{40}\text{H}_{34}\text{BF}_2\text{N}_3\text{O}_2^+$ , Calcd: 637.3; Obsd: 637.3.

**2.3. CBZ-BOD@ZIF-8.** 2-Methylimidazole (0.657 g, 8.000 mmol) was dissolved in 5 mL of deionized water in a round-bottom flask, followed by addition of CBZ-BOD (0.015 g, 0.023 mmol) and then ultrasonic dissolution. A fresh zinc acetate dihydrate (0.088 g, 0.400 mmol) solution was prepared using 5 mL of deionized water, then added to the mixture. The final mixture solution was left standing for 12 h. After that, the mixture was centrifuged for 6 min (10,000 rpm). The precipitation was collected, washed with 20 mL of ethanol, and centrifuged again. After several times of washing, the supernatant after centrifugation is colorless, and the precipitate is collected.<sup>34</sup> The product is obtained after vacuum drying.

**2.4. Chlorpyrifos Titration Experiment.** Chlorpyrifos (from 0 to 8  $\mu$ M) was first incubated with CES1 (10  $\mu$ g/mL) for 30 min in 200  $\mu$ L of phosphate-buffered saline (PBS) buffer (100 mM, pH 7.4), and then, CBZ-BOD@ZIF-8 (maintain at 10  $\mu$ M) was added and incubated for another 60 min. After that, 200  $\mu$ L of  $\text{CH}_3\text{CN}$  was added to quench the reaction, and the mixture solution was used to measure the fluorescence intensity.

**2.5. Molecular Docking Study.** AutoDock 4.2 with the Lamarckian genetic algorithm was used for molecular docking to construct the complex structure of small molecules and CES1. Targeting the CES1 receptor, the potential active site identified by the AlloSite online server in the CES1 crystal structure (PDB code: 4AB1) was used as the center of the grid box for docking, and the size of the grid box was 22.5  $\times$  22.5  $\times$  22.5 Å. Pretreatment of the small molecule and receptor structure for docking was carried out with the

**Scheme 2. Synthesis of CBZ-BOD and Its Application in CES1 Detection; (a) Synthetic Route of CBZ-BOD; and (b) Detection Process of CBZ-BOD in the Process of CES1**



AutoDockTools program suite. The small molecules were set as flexible structures, and CES1 was regarded as a rigid structure. Two hundred independent docking runs were conducted for each small molecule to the receptor structure. To perform the Lamarckian genetic algorithm, a population of 150 random small molecule conformations in random orientations and at random translations was first generated, and then, the population evolved according to the algorithm and was terminated after 27,000 generations and a maximum of 1,500,000 energy evaluations. Other parameters for running the program were set to default values in the AutoDock program. After the molecular docking is completed, the scoring function provided by AutoDock 4.2 was used to evaluate the docking results, and the lowest energy position of each small molecule with the best docking score was adopted. Finally, the protein–ligand interaction profiler online server was used to analyze the intermolecular interaction of the best binding conformation.

### 3. RESULT AND DISCUSSION

**3.1. Design and Synthesis of CBZ-BOD and CBZ-BOD@ZIF-8.** Herein, we first synthesized a red emission probe CBZ-BOD for detecting CES1 via a enzyme-catalyzed hydrolysis reaction. The synthesis process of CBZ-BOD is shown in Scheme 2a; the electron donating group *N*-ethyl-3-carbazolecarboxaldehyde was conjugated to the BODIPY fluorophore to realize the red emission.<sup>35–37</sup> Thereafter, benzoyl chloride was introduced to BOD-OH as a reactive moiety through an ester bond. CBZ-BOD can specifically bind with CES1 and is accompanied with significant fluorescence changes (Scheme 2b). Finally, to improve the detection property of CBZ-BOD, ZIF-8 was chosen as the framework to prepare BOD-OH@ZIF-8. This novel probe materialization technology can significantly improve the detection performance of the probe.

**3.2. Characterization of CBZ-BOD@ZIF-8.** To confirm that CBZ-BOD@ZIF-8 was successfully synthesized, scanning

electron microscopy (SEM) and X-ray powder diffraction (XRD) were used to characterize the material. The results are shown in Figure 1; SEM images of CBZ-BOD@ZIF-8 exhibit the typical topography of ZIF-8, from which we can see that

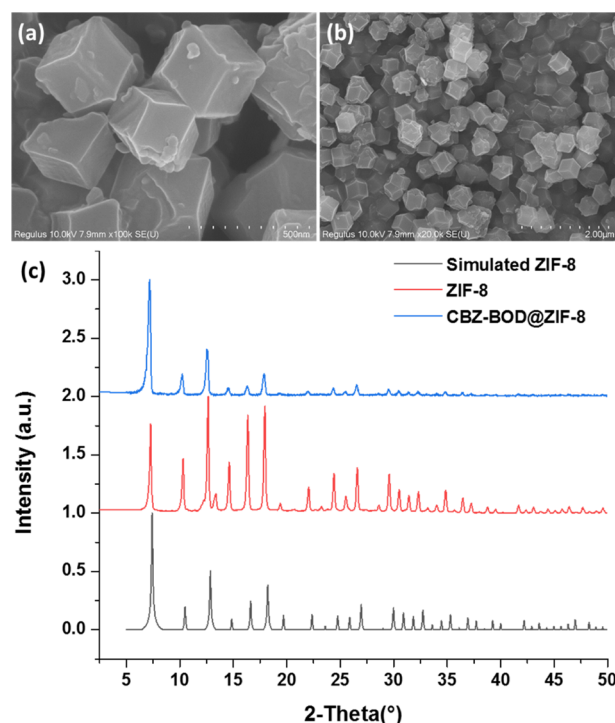


**Figure 1.** Characterization of CBZ-BOD@ZIF-8. (a,b) SEM images of CBZ-BOD@ZIF-8; (c) XRD patterns of simulated ZIF-8 (black line), fresh ZIF-8 (red line), and CBZ-BOD@ZIF-8.

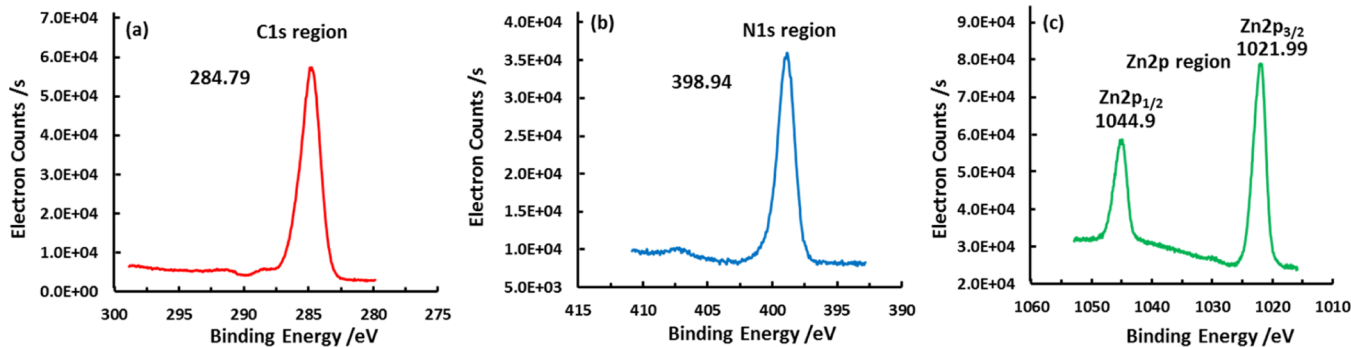


**Figure 2.** XPS data of CBZ-BOD@ZIF-8 in different regions. (a) C 1s region; (b) N 1s region; and (c) Zn 2p region.

out shape of CBZ-BOD@ZIF-8 with regular edges and corners. The XRD pattern was also investigated, as shown in Figure 1c. Here, fresh ZIF-8 was prepared and measured first; the data were compared to that of simulated ZIF-8 and exhibited good consistency. Then, CBZ-BOD@ZIF-8 was prepared using the same method; these data are finally summarized and compared, and they exhibited good consistency and reproducibility, demonstrating that CBZ-BOD@ZIF-8 was successfully synthesized. The encapsulation efficiency was calculated to be 75.9% (Figure S7).

The structure of CBZ-BOD@ZIF-8 was further confirmed by X-ray photoelectron spectroscopy (XPS), and the results are shown in Figure 2. A signal peak can be observed in Figure 2a; this peak (284.79 eV) corresponds to C of the ligand. The peak at 398.94 eV of Figure 2b is attributed to N of the ligand. Lastly, two signal peaks at 1021.99 eV (Zn 2p<sub>3/2</sub>) and 1044.9 eV (Zn 2p<sub>1/2</sub>) in the zinc region (Figure 2c) are compatible with Zn<sup>2+</sup> of the ZIF-8 structure.

**3.3. Photophysical Properties and Quantitative Determination of CES1 and Chlorpyrifos.** Considering the importance of the basic physical properties, we first investigated the absorption and fluorescence spectrum of CBZ-BOD (Figures S1 and S2). The maximum absorption wavelength was observed at 585 nm, and the corresponding maximum emission wavelength was located at 624 nm. Obviously, it is a red emission probe, and the Stokes shift was calculated as 39 nm, which renders the probe low background noise upon detecting biological samples. Basic absorption and emission spectra of CBZ-BOD@ZIF-8 were also investigated, finding that the maximum absorption and emission wavelength remained almost unchanged (Figures S3 and S4). Selectivity analysis of CBZ-BOD@ZIF-8 to CES1 was then carried out. Fluorescence responses of CBZ-BOD@ZIF-8 in the presence of various potential interfering species including CES1, CES2,  $\alpha$ -CT, trypsin, lysing enzymes, lipase, proteinase K, HSA, pepsase, BSA, BHB, lysozyme, AchE, and BchE were measured, and the results are displayed in Figure 3a. The data showed that both CES1 and CES2 can catalyze the hydrolysis of the carboxylic ester bond in the probe CBZ-BOD. In contrast, however, CES1 appears to be more capable of hydrolyzing CBZ-BOD than CES2. Besides, no significant changes can be observed in other interfering species. The results demonstrated that CBZ-BOD@ZIF-8 exhibited a relatively good specific response to CES1.

We then investigated the fluorescence intensity changes with different CES1 incubation times. As shown in Figure 3b, obviously the fluorescence intensity of CBZ-BOD@ZIF-8 decreases with the extension of the CES1 incubation time,

indicating that CBZ-BOD@ZIF-8 slowly adopted to conformation, decreasing the fluorescence emission upon hydrolysis by CES1. Here, the Michaelis constants ( $K_m$ ) and the catalytic constants ( $K_{cat}$ ) were determined according to the standard test method, and the results are listed in Table 1. Actually, in CBZ-BOD@ZIF-8, the micropores of the MOF structure served as a microreactor, and the probe molecules are more concentrated in the MOF material, which greatly improves the reaction efficiency of enzymatic hydrolysis. The detection sensitivity of CBZ-BOD was greatly improved.

To figure out if CBZ-BOD@ZIF-8 can be used for quantitative detection of CES1, an enzyme activity titration experiment was carried out. As shown in Figure 3c, from which we can easily find that the fluorescence intensity of CBZ-BOD@ZIF-8 exhibited a decreasing trend with the increasing concentration of CES1. We find that the fluorescence intensity of CBZ-BOD@ZIF-8 remains unchanged when the concentration is over 10  $\mu$ g/mL. The fluorescence intensity of CBZ-BOD@ZIF-8 exhibited a good linearity with the concentration changes in the range of 1–6  $\mu$ g/mL (Figure 3d). The LOD was calculated as 1.15 ng/mL.<sup>38–40</sup> Compared with the existing literature (Table S6), the LOD of CBZ-BOD@ZIF-8 for CES1 is superior to those reported. The results demonstrate that CBZ-BOD@ZIF-8 can be used to quantitatively detect CES1.

Chlorpyrifos are potential inhibitors of esterase; therefore, a pesticide titration experiment was carried out to confirm if CBZ-BOD@ZIF-8 can serve as the indicator for pesticide residues. As shown in Figure 3e, CES1 was first pre-incubated with different chlorpyrifos concentrations for 30 min, and then, CBZ-BOD@ZIF-8 was added and incubated for 60 min. Interestingly, the fluorescence intensity of CBZ-BOD@ZIF-8 displayed an increasing tendency with the rising chlorpyrifos concentration because with the increase in chlorpyrifos concentration, the CES1 activity was inhibited. The fluorescence intensity increased 2.59-fold, and a good linear relationship was observed in the range of 1–8  $\mu$ M. The results demonstrate that CBZ-BOD@ZIF-8 can be used as a quantitative indicator of chlorpyrifos residues. In general, the LODs of CBZ-BOD@ZIF-8 and CBZ-BOD in the determination of CES1 and chlorpyrifos were calculated. The LODs for CES1 were 1.15 ng/mL for CBZ-BOD@ZIF-8 and 1.47  $\mu$ g/mL for CBZ-BOD. Additionally, the LODs for chlorpyrifos were 0.16  $\mu$ M for CBZ-BOD@ZIF-8 and 0.44  $\mu$ M for CBZ-BOD. Obviously, CBZ-BOD@ZIF-8 is superior to CBZ-BOD in the determination of CES1 and chlorpyrifos. To confirm if other organophosphorus pesticides can be detected by CBZ-BOD@ZIF-8, a contrast experiment was carried out using

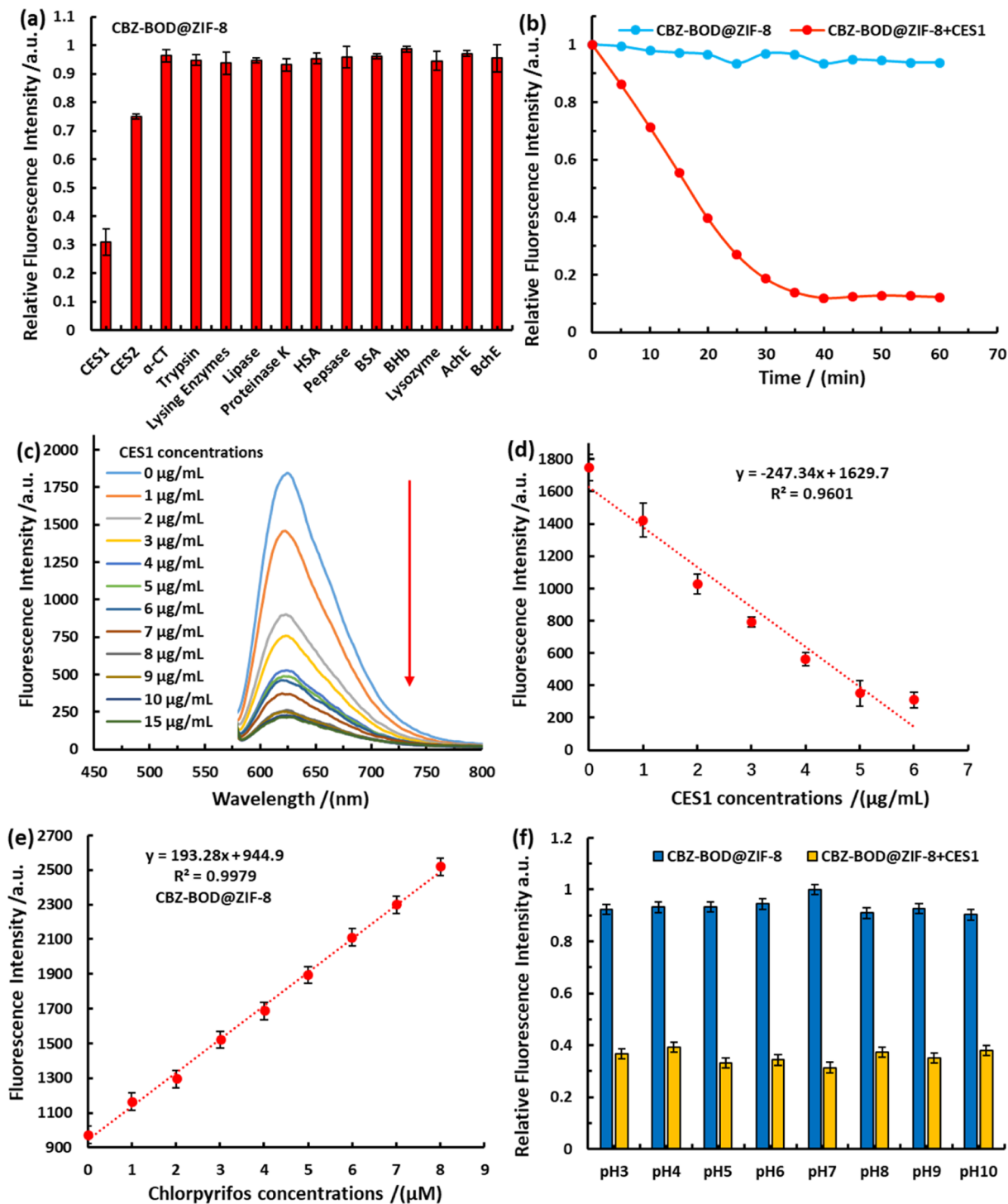


**Figure 3.** Quantitative detection properties of CBZ-BOD@ZIF-8 toward CES1. (a) Selectivity: relative fluorescence intensity of CBZ-BOD@ZIF-8 incubated with different enzymes ( $50 \mu\text{g}/\text{mL}$ ); (b) relative fluorescence intensity changes of CBZ-BOD@ZIF-8 ( $10 \mu\text{M}$ ) with different CES1 ( $20 \mu\text{g}/\text{mL}$ ) incubation times; (c) titration experiment: fluorescence changes of CBZ-BOD@ZIF-8 ( $10 \mu\text{M}$ ) in the presence of different concentrations of CES1; (d) fitting plot of (c); (e) relative fluorescence intensity changes of CBZ-BOD@ZIF-8 in the presence of different chlorpyrifos concentrations; and (f) relative fluorescence intensity of CBZ-BOD@ZIF-8 ( $10 \mu\text{M}$ ) in different pH PBS buffer solutions before and after incubation with CES1 ( $10 \mu\text{g}/\text{mL}$ ).

**Table 1. Kinetic Parameters of CBZ-BOD@ZIF-8 Catalyzed by CES1**

parameters	$K_m (\mu\text{M})$	$V_{max} (\mu\text{M}\cdot\text{s}^{-1})$	$K_{cat} (\text{s}^{-1})$	$K_{cat}/K_m (\text{M}^{-1}\cdot\text{s}^{-1})$
CES1	46.86	329.03	3.29	$7.02 \times 10^4$

chlorpyrifos, dimethoate, and fenitrothion. As shown in Figure S8, although CBZ-BOD@ZIF-8 is responsive to other organophosphorus pesticides, it has the best response to chlorpyrifos. Actually, pH stability is also of great significance for the normal detection of a specific target. Thus, we further investigated the pH stability of CBZ-BOD@ZIF-8 and CBZ-

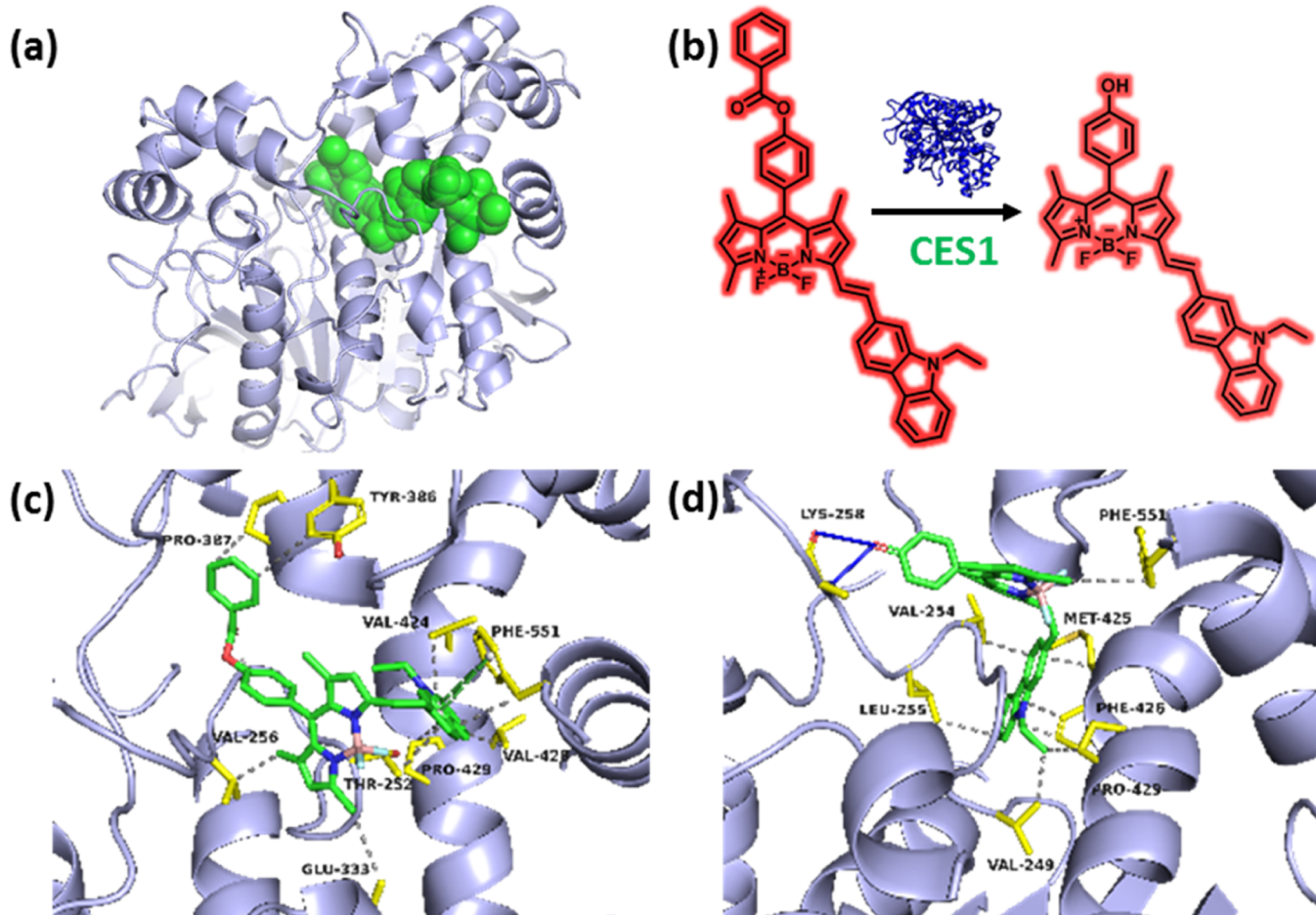


**Figure 4.** (a) AlloSite-predicted potential binding site (green color) in CES1 (PDB: 4AB1); (b) CBZ-BOD before and after being hydrolyzed by CES1; and (c,d) interaction of CBZ-BOD (c) and hydrolyzed CBZ-BOD (d) with CES1; the blue solid line indicates hydrogen bonding and the gray dotted line indicates hydrophobic interaction. Yellow stick models are amino acid residues, and the green stick model is CBZ-BOD or hydrolyzed CBZ-BOD.

BOD. As shown in Figures 3f and S6, although CBZ-BOD exhibits a relatively good pH tolerability, the pH stability of CBZ-BOD@ZIF-8 is still superior to that of CBZ-BOD before and after reacting with CES1 in a wide pH range since the relative fluorescence intensity of CBZ-BOD@ZIF-8 in different pH solutions before and after being incubated with CES1 almost has no changes, which suggests that CBZ-BOD@ZIF-8 has good pH stability. We also investigated the stability of CBZ-BOD@ZIF-8 in aqueous solutions; CBZ-BOD@ZIF-8 was added to the aqueous solutions of different pH values, and then, the fluorescence intensity changes were recorded every 5 min by a microplate reader. As the results show in Figure S9, almost no fluorescence changes can be observed over a long period of time, demonstrating that CBZ-BOD@ZIF-8 has good stability in aqueous solutions.

**3.4. Molecular Docking Study.** AlloSite only identified one potential active/binding site in the target protein CES1, which is the pocket marked in green (Figure 4a). The pocket druggability score is as high as 0.93 (as shown in Table S1). The pocket volume and pocket total solvent available surface area are 1111.65 and 594.45, respectively. The steps are to set a  $60 \times 60 \times 60$  step docking square box (step length 0.375 Å) at the potential binding site of the target protein CES1 (PDB: 4AB1) predicted by AlloSite and perform 200 times independent docking for the target small molecules before

and after hydrolysis (Tables S2 and S3). After the docking is completed, the best binding conformations of two small molecules are selected from the best clusters, and the scores are -11.16 and -12.1 respectively. From the scoring, CBZ-BOD and hydrolyzed CBZ-BOD can bind to the CES1 stably (Figure 4c,d). The benzoyl group of CBZ-BOD is oxidized and dissociated and leads to the hydrolyzed CBZ-BOD losing the interaction at the active sites TYR386 and PRO387, resulting in the changes of the binding mode of active sites before and after hydrolysis. The dibenzopyrrole structure of hydrolyzed CBZ-BOD can interact with LEU255 and PHE426 in the deeper active site, while the dibenzopyrrole structure of CBZ-BOD interacts with PHE551 and VAL428 (Tables S4 and S5).

**3.5. Monitor the Real Time Activity of CES1 in Living Cells.** In this work, CBZ-BOD@ZIF-8 was applied to the visual detection of CES1 activities in living cells, and HepG2 cells were used.<sup>41–43</sup> To explore the effect of the probe and chlorpyrifos on the cell state, a cell cytotoxicity test of the probe and chlorpyrifos was conducted before the cell imaging experiment (Figures S5 and S10), and the results showed that the low concentrations of CBZ-BOD as well as chlorpyrifos used in the experiment almost had no effect on the cell state; HepG2 cells still retain high activity. Then, the visual detection experiment in HepG2 cells was carried out. As shown in Figure 5a–d, if HepG2 cells are only co-stained with the nuclear dye

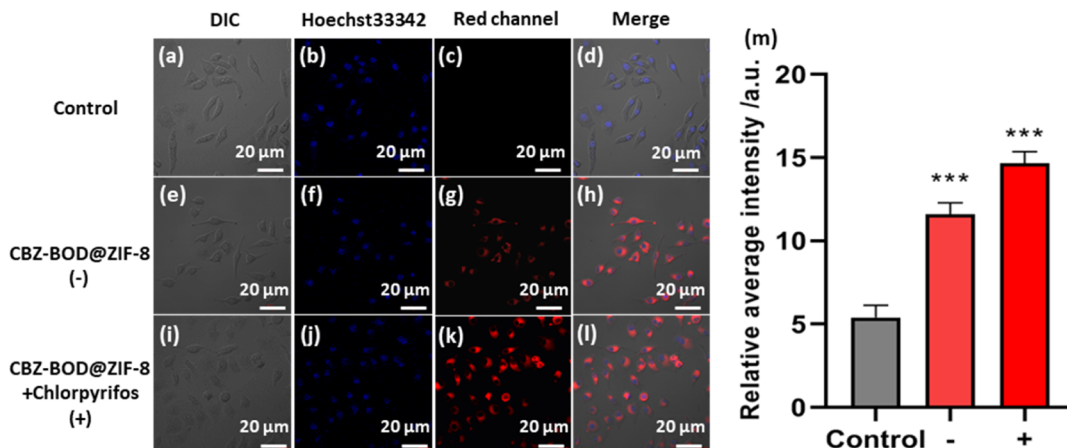


**Figure 5.** Living cell images of CBZ-BOD@ZIF-8. (a–d) Control experiment: HepG2 cells just stained with the Hoechst 33342 (10  $\mu$ M); (e–h) HepG2 cells co-stained with Hoechst 33342 and CBZ-BOD@ZIF-8 (10  $\mu$ M); (i–l) HepG2 cells were pretreated with chlorpyrifos (5  $\mu$ M) and then co-stained with Hoechst 33342 (10  $\mu$ M) and CBZ-BOD@ZIF-8 (10  $\mu$ M); and (m) average intensity of cell images in the red channel. Scale bar = 20  $\mu$ m.

Hoechst 33342 (10  $\mu$ M), only blue fluorescence can be observed in the blue channel. However, if HepG2 cells were co-stained by CBZ-BOD@ZIF-8 (10  $\mu$ M) and Hoechst 33342 (10  $\mu$ M) for 30 min and then observed under laser scanning confocal microscopy, a red fluorescence signal can be observed (Figure 5g). Nonetheless, if HepG2 cells were pretreated with 5  $\mu$ M chlorpyrifos for 30 min and then incubated with both Hoechst 33342 as well as CBZ-BOD@ZIF-8 for 30 min, a fluorescence enhancement in the red channel can be observed (Figure 5k) because the activity of carboxylesterase was inhibited by chlorpyrifos. The results suggest that CBZ-BOD@ZIF-8 is a good bioimaging reagent for monitoring CES1 in living cells.

#### 4. CONCLUSIONS

In general, a novel red emission CES1 probe CBZ-BOD was designed and synthesized, and also, we provide a method for constructing sensitivity detection materials based on MOFs. Here, CBZ-BOD@ZIF-8 was prepared and successfully applied to the quantitative determination of CES1 activity. Besides, CBZ-BOD@ZIF-8 can also serve as a fluorescence indicator of pesticide exposure in the way of hydrolyzing the carboxylic acid ester group in CBZ-BOD. The low LOD of CBZ-BOD@ZIF-8 in the presence of CES1 was calculated as 1.15 ng/mL. CBZ-BOD@ZIF-8 has excellent stability, better pH tolerability, and a high fluorescence quantum yield (0.65). Visual monitoring of CES1 in living cells was realized using CBZ-BOD@ZIF-8. The successful design of CBZ-BOD@ZIF-8 has a certain significance for the development of specific enzyme probes as well as pesticide detection tools.

#### ■ ASSOCIATED CONTENT

##### SI Supporting Information

The Supporting Information is available free of charge at <https://pubs.acs.org/doi/10.1021/acsami.0c19811>.

Experimental details, basic absorption and fluorescence spectra of CBZ-BOD and CBZ-BOD@ZIF-8, cytotoxicity of CBZ-BOD, pH stability of CBZ-BOD, determination of encapsulation efficiency, fluorescence quantum yield measurement, fluorescence response of CBZ-BOD@ZIF-8 to different pesticides, stability of CBZ-BOD@ZIF-8, cytotoxicity of chlorpyrifos, mass

spectra of BOD-OH and CBZ-BOD, fluorescence quantum yield measurement, molecular docking study, and comparison with other reported CES1 probes (PDF)

#### ■ AUTHOR INFORMATION

##### Corresponding Authors

Baoxing Shen – School of Food Science and Pharmaceutical Engineering, Nanjing Normal University, Nanjing, Jiangsu 210023, China; orcid.org/0000-0002-5399-8105; Email: [shenbx@njnu.edu.cn](mailto:shenbx@njnu.edu.cn)

Xing Zhang – School of Food Science and Pharmaceutical Engineering, Nanjing Normal University, Nanjing, Jiangsu 210023, China; Email: [zhangxing@njnu.edu.cn](mailto:zhangxing@njnu.edu.cn)

He Huang – School of Food Science and Pharmaceutical Engineering, Nanjing Normal University, Nanjing, Jiangsu 210023, China; Email: [huangh@njnu.edu.cn](mailto:huangh@njnu.edu.cn)

##### Authors

Chenggong Ma – School of Food Science and Pharmaceutical Engineering, Nanjing Normal University, Nanjing, Jiangsu 210023, China

Yuan Ji – School of Food Science and Pharmaceutical Engineering, Nanjing Normal University, Nanjing, Jiangsu 210023, China

Jianan Dai – School of Food Science and Pharmaceutical Engineering, Nanjing Normal University, Nanjing, Jiangsu 210023, China

Bingzhi Li – School of Food Science and Pharmaceutical Engineering, Nanjing Normal University, Nanjing, Jiangsu 210023, China; orcid.org/0000-0002-5533-2147

Complete contact information is available at:  
<https://pubs.acs.org/10.1021/acsami.0c19811>

##### Notes

The authors declare no competing financial interest.

#### ■ ACKNOWLEDGMENTS

This work was financially supported by the “Youth Program of National Natural Science Foundation” of China (grant no. 22007048 & 22007049), the Natural Science Foundation of Jiangsu Province (BK20200728), Jiangsu Specially-Appointed

Professor Project to X.Z., the Natural Science Foundation of the Jiangsu Higher Education Institutions of China (20KJB150046), the Science and Technology Innovation Project for Overseas Students of Nanjing in 2020 (184080H201148), and the Jiangsu innovation and entrepreneurship doctoral program to B.S.

## ■ REFERENCES

- (1) Dong, Y.; Zheng, W.; Chen, D.; Li, X.; Wang, J.; Wang, Z.; Chen, Y. Click Reaction-Mediated T2 Immunosensor for Ultra-sensitive Detection of Pesticide Residues via Brush-like Nanostructure-Triggered Coordination Chemistry. *J. Agric. Food Chem.* **2019**, *67*, 9942–9949.
- (2) Huang, S.; Yao, J.; Chu, X.; Liu, Y.; Xiao, Q.; Zhang, Y. One-Step Facile Synthesis of Nitrogen-Doped Carbon Dots: A Ratiometric Fluorescent Probe for Evaluation of Acetylcholinesterase Activity and Detection of Organophosphorus Pesticides in Tap Water and Food. *J. Agric. Food Chem.* **2019**, *67*, 11244–11255.
- (3) Li, D.; Li, Z.; Chen, W.; Yang, X. Imaging and Detection of Carboxylesterase in Living Cells and Zebrafish Pretreated with Pesticides by a New Near-Infrared Fluorescence Off-On Probe. *J. Agric. Food Chem.* **2017**, *65*, 4209–4215.
- (4) Liu, J.; Xiong, W. H.; Ye, L. Y.; Zhang, W. S.; Yang, H. Developing a Novel Nanoscale Porphyrinic Metal-Organic Framework: A Bifunctional Platform with Sensitive Fluorescent Detection and Elimination of Nitenpyram in Agricultural Environment. *J. Agric. Food Chem.* **2020**, *68*, 5572–5578.
- (5) Yang, L.; Liu, Y.-L.; Liu, C.-G.; Ye, F.; Fu, Y. Two Luminescent Dye@MOFs Systems as Dual-Emitting Platforms for Efficient Pesticides Detection. *J. Hazard. Mater.* **2020**, *381*, 120966.
- (6) Song, D.; Jiang, X.; Li, Y.; Lu, X.; Luan, S.; Wang, Y.; Li, Y.; Gao, F. Metal-organic frameworks-derived MnO<sub>2</sub>/Mn<sub>3</sub>O<sub>4</sub> microcuboids with hierarchically ordered nanosheets and Ti<sub>3</sub>C<sub>2</sub> MXene/Au NPs composites for electrochemical pesticide detection. *J. Hazard. Mater.* **2019**, *373*, 367–376.
- (7) Tu, X.; Gao, F.; Ma, X.; Zou, J.; Yu, Y.; Li, M.; Qu, F.; Huang, X.; Lu, L. Mxene/carbon nanohorn/β-cyclodextrin-Metal-organic frameworks as high-performance electrochemical sensing platform for sensitive detection of carbendazim pesticide. *J. Hazard. Mater.* **2020**, *396*, 122776.
- (8) Lin, B.; Yan, Y.; Guo, M.; Cao, Y.; Yu, Y.; Zhang, T.; Huang, Y.; Wu, D. Modification-free Carbon Dots as Turn-on Fluorescence Probe for Detection of Organophosphorus Pesticides. *Food Chem.* **2018**, *245*, 1176–1182.
- (9) Carullo, P.; Chino, M.; Cetrangolo, G. P.; Terreri, S.; Lombardi, A.; Manco, G.; Cimmino, A.; Febbraio, F. Direct Detection of Organophosphate Compounds in Water by a Fluorescence-based Biosensing Device. *Sens. Actuators, B* **2018**, *255*, 3257–3266.
- (10) Shakourian, M.; Yamini, Y.; Safari, M. Facile Magnetization of Metal-organic Framework TMU-6 for Magnetic Solid-phase Extraction of Organophosphorus Pesticides in Water and Rice Samples. *Talanta* **2020**, *218*, 121139.
- (11) Bala, R.; Dhingra, S.; Kumar, M.; Bansal, K.; Mittal, S.; Sharma, R. K.; Wangoo, N. Detection of Organophosphorus Pesticide—Malathion in Environmental Samples Using Peptide and Aptamer Based Nanoprobes. *Chem. Eng. J.* **2017**, *311*, 111–116.
- (12) Chang, M. M. F.; Ginjom, I. R.; Ng, S. M. Single-shot “Turn-off” Optical Probe for Rapid Detection of Paraoxon-ethyl Pesticide on Vegetable Utilising Fluorescence Carbon Dots. *Sens. Actuators, B* **2017**, *242*, 1050–1056.
- (13) Shi, J.; Deng, Q.; Li, Y.; Zheng, M.; Chai, Z.; Wan, C.; Zheng, Z.; Li, L.; Huang, F.; Tang, B. A Rapid and Ultrasensitive Tetraphenylethylene-Based Probe with Aggregation-Induced Emission for Direct Detection of α-Amylase in Human Body Fluids. *Anal. Chem.* **2018**, *90*, 13775–13782.
- (14) Tseng, M.-H.; Hu, C.-C.; Chiu, T.-C. A Fluorescence Turn-on Probe for Sensing Thiodicarb Using Rhodamine B Functionalized Gold Nanoparticles. *Dyes Pigm.* **2019**, *171*, 107674.
- (15) Champagne, P.-L.; Kumar, R.; Ling, C.-C. Multi-responsive self-assembled pyrene-appended β-cyclodextrin nanoaggregates: Discriminative and selective ratiometric detection of pirimicarb pesticide and trinitroaromatic explosives. *Sens. Actuators, B* **2019**, *281*, 229–238.
- (16) Miliutina, E.; Guselnikova, O.; Burtsev, V.; Elashnikov, R.; Postnikov, P.; Svorcik, V.; Lyutakov, O. Plasmon-active Optical Fiber Functionalized by Metal Organic Framework for Pesticide Detection. *Talanta* **2020**, *208*, 120480.
- (17) Zhang, X.; Lin, L.; Huang, H.; Linhardt, R. J. Chemoenzymatic Synthesis of Glycosaminoglycans. *Acc. Chem. Res.* **2020**, *53*, 335–346.
- (18) Li, B.; Xu, L.; Chen, Y.; Zhu, W.; Shen, X.; Zhu, C.; Luo, J.; Li, X.; Hong, J.; Zhou, X. Sensitive and Label-Free Fluorescent Detection of Transcription Factors Based on DNA-Ag Nanoclusters Molecular Beacons and Exonuclease III-Assisted Signal Amplification. *Anal. Chem.* **2017**, *89*, 7316–7323.
- (19) Liu, S.-Y.; Qu, R.-Y.; Li, R.-R.; Yan, Y.-C.; Sun, Y.; Yang, W.-C.; Yang, G.-F. An Activity-Based Fluorogenic Probe Enables Cellular and in Vivo Profiling of Carboxylesterase Isozymes. *Anal. Chem.* **2020**, *92*, 9205–9213.
- (20) Tian, X.; Yan, F.; Zheng, J.; Cui, X.; Feng, L.; Li, S.; Jin, L.; James, T. D.; Ma, X. Endoplasmic Reticulum Targeting Ratiometric Fluorescent Probe for Carboxylesterase 2 Detection in Drug-Induced Acute Liver Injury. *Anal. Chem.* **2019**, *91*, 15840–15845.
- (21) Li, B.; Chen, Y.; Wang, J.; Lu, Q.; Zhu, W.; Luo, J.; Hong, J.; Zhou, X. Detecting Transcription Factors with Allosteric DNA-Silver Nanocluster Switches. *Anal. Chim. Acta* **2019**, *1048*, 168–177.
- (22) Lin, L.; Yu, Y.; Zhang, F.; Xia, K.; Zhang, X.; Linhardt, R. J. Bottom-up and Top-down Profiling of Pentosan Polysulfate. *Analyst* **2019**, *144*, 4781–4786.
- (23) Feng, J.; Xu, Y.; Huang, W.; Kong, H.; Li, Y.; Cheng, H.; Li, L. A Magnetic SERS Immunosensor for Highly Sensitive and Selective Detection of Human Carboxylesterase 1 in Human Serum Samples. *Anal. Chim. Acta* **2020**, *1097*, 176–185.
- (24) Jiang, A.; Chen, G.; Xu, J.; Liu, Y.; Zhao, G.; Liu, Z.; Chen, T.; Li, Y.; James, T. D. Ratiometric Two-photon Fluorescent Probe for in Situ Imaging of Carboxylesterase (CE)-mediated Mitochondrial Acidification During Medication. *Chem. Commun.* **2019**, *55*, 11358–11361.
- (25) Ghiasi, A.; Malekpour, A.; Mahpishanian, S. Metal-organic Framework MIL101 (Cr)-NH<sub>2</sub> Functionalized Magnetic Graphene Oxide for Ultrasonic-assisted Magnetic Solid Phase Extraction of Neonicotinoid Insecticides from Fruit and Water Samples. *Talanta* **2020**, *217*, 121120.
- (26) Zhang, F.; Liu, Y.; Ma, P.; Tao, S.; Sun, Y.; Wang, X.; Song, D. A Mn-doped ZnS Quantum Dots-based Ratiometric Fluorescence Probe for Lead Ion Detection and “Off-on” Strategy for Methyl Parathion Detection. *Talanta* **2019**, *204*, 13–19.
- (27) Xue, L.; Qian, X.; Jin, Q.; Zhu, Y.; Wang, X.; Wang, D.; Ge, G.; Yang, L. Construction and Application of a High-content Analysis for Identifying Human Carboxylesterase 2 Inhibitors in Living Cell System. *Anal. Bioanal. Chem.* **2020**, *412*, 2645–2654.
- (28) Tian, Z.; Ding, L.; Li, K.; Song, Y.; Dou, T.; Hou, J.; Tian, X.; Feng, L.; Ge, G.; Cui, J. Rational Design of a Long-Wavelength Fluorescent Probe for Highly Selective Sensing of Carboxylesterase 1 in Living Systems. *Anal. Chem.* **2019**, *91*, 5638–5645.
- (29) Gardner, S. H.; Reinhardt, C. J.; Chan, J. Advances in Activity-Based Sensing Probes for Isoform-Selective Imaging of Enzymatic Activity. *Angew. Chem., Int. Ed.* **2020**, DOI: 10.1002/anie.202003687.
- (30) Xiao, M.; Fan, J.; Li, M.; Xu, F.; Zhao, X.; Xi, D.; Ma, H.; Li, Y.; Du, J.; Sun, W.; Peng, X. A Photosensitizer-inhibitor Conjugate for Photodynamic Therapy with Simultaneous Inhibition of Treatment Escape Pathways. *Biomaterials* **2020**, *257*, 120262.
- (31) Xiang, H.-J.; Tham, H. P.; Nguyen, M. D.; Fiona Phua, S. Z.; Lim, W. Q.; Liu, J.-G.; Zhao, Y. An Aza-BODIPY Based Near-infrared Fluorescent Probe for Sensitive Discrimination of Cysteine/homocysteine and Glutathione in living cells. *Chem. Commun.* **2017**, *53*, 5220–5223.

- (32) Wang, Y.; Yu, F.; Luo, X.; Li, M.; Zhao, L.; Yu, F. Visualization of Carboxylesterase 2 with a Near-infrared Two-photon Fluorescent Probe and Potential Evaluation of Its Anticancer Drug Effects in an Orthotopic Colon Carcinoma Mice Model. *Chem. Commun.* **2020**, *56*, 4412–4415.
- (33) Kailass, K.; Sadovski, O.; Capello, M.; Kang, Y. a.; Fleming, J. B.; Hanash, S. M.; Beharry, A. A. Measuring Human Carboxylesterase 2 Activity in Pancreatic Cancer Patient-derived Xenografts Using a Ratiometric Fluorescent Chemosensor. *Chem. Sci.* **2019**, *10*, 8428–8437.
- (34) Zou, R.; Gong, Q.; Shi, Z.; Zheng, J.; Xing, J.; Liu, C.; Jiang, Z.; Wu, A. A ZIF-90 Nanoplatform Loaded with an Enzyme-responsive Organic Small-molecule Probe for Imaging the Hypoxia Status of Tumor Cells. *Nanoscale* **2020**, *12*, 14870–14881.
- (35) Huang, L.; Duan, R.; Li, Z.; Zhang, Y.; Zhao, J.; Han, G. BODIPY-Based Nanomicelles as Near-Infrared Fluorescent “Turn-On” Sensors for Biogenic Thiols. *ChemNanoMat* **2016**, *2*, 396–399.
- (36) Liu, X.; Li, X.; Dong, P.; Wu, Z.; Gao, J.; Wang, Q. Near-infrared Emission Tracks Inter-Individual Variability of Carboxylesterase-2 via a Novel Molecular Substrate. *Microchim. Acta* **2020**, *187*, 313.
- (37) Shen, B.; Wang, L. F.; Zhi, X.; Qian, Y. Construction of a Red Emission BODIPY-based Probe for Tracing Lysosomal Viscosity Changes in Culture Cells. *Sens. Actuators, B* **2020**, *304*, 127271.
- (38) Liu, Z.-m.; Du, H.-j.; Wang, T.-q.; Ma, Y.-n.; Liu, J.-r.; Yan, M.-c.; Wang, H.-y. Selective and Sensitive Detection and Quantification of Human Carboxylesterase 1 by a Ratiometric Fluorescence Probe. *Dyes Pigm.* **2019**, *171*, 107711.
- (39) Song, Y.-Q.; Guan, X.-Q.; Weng, Z.-M.; Wang, Y.-Q.; Chen, J.; Jin, Q.; Fang, S.-Q.; Fan, B.; Cao, Y.-F.; Hou, J.; Ge, G.-B. Discovery of a Highly Specific and Efficacious Inhibitor of Human Carboxylesterase 2 by Large-scale Screening. *Int. J. Biol. Macromol.* **2019**, *137*, 261–269.
- (40) Zhou, H.; Tang, J.; Zhang, J.; Chen, B.; Kan, J.; Zhang, W.; Zhou, J.; Ma, H. A Red Lysosome-Targeted Fluorescent Probe for Carboxylesterase Detection and Bioimaging. *J. Mater. Chem. B* **2019**, *7*, 2989–2996.
- (41) Zhou, L.; Kang, Q.; Fang, M.; Yu, L. Label-free, Rapid, and Sensitive Detection of Carboxylesterase Using Surfactant-doped Liquid Crystal Sensor. *J. Mol. Liq.* **2019**, *296*, 111921.
- (42) Zhang, X.; Han, X.; Xia, K.; Xu, Y.; Yang, Y.; Oshima, K.; Haeger, S. M.; Perez, M. J.; McMurtry, S. A.; Hippenstein, J. A.; Ford, J. A.; Herson, P. S.; Liu, J.; Schmidt, E. P.; Linhardt, R. J. Circulating Heparin Oligosaccharides Rapidly Target the Hippocampus in Sepsis, Potentially Impacting Cognitive Functions. *Proc. Natl. Acad. Sci. U.S.A.* **2019**, *116*, 9208–9213.
- (43) Li, B.; Chen, Y.; Wang, J.; Lu, Q.; Zhu, W.; Xu, L.; Shen, X.; Luo, J.; Zhu, C.; Li, X.; Hong, J.; Zhou, X. DNA-silver Nanoclusters/polypyrrole Nanoparticles: A Label-free and Enzyme-free Platform for Multiplexed Transcription Factors Detection. *Sens. Actuators, B* **2018**, *274*, 481–490.